Biochemistry

 Volume 39, Number 10 March 14, 2000

Articles

Effects of Subunit Occupancy on Partitioning of an Intermediate in Thymidylate Synthase Mutants†

Prasanna Variath, Yaoquan Liu, Tom T. Lee, Robert M. Stroud, and Daniel V. Santi*

Departments of Biochemistry and Biophysics and Pharmaceutical Chemistry, University of California, San Francisco, California 94143-0448

Received August 3, 1999; Revised Manuscript Received December 8, 1999

ABSTRACT: Experimental evidence for a 5-exocyclic methylene-dUMP intermediate in the thymidylate synthase reaction was recently obtained by demonstrating that tryptophan 82 mutants of the *Lactobacillus casei* enzyme produced 5-(2-hydroxyethyl)thiomethyl-dUMP (HETM-dUMP) (Barret, J. E., Maltby, D. A., Santi, D. V., and Schultz, P. G. (1998) *J. Am. Chem. Soc. 120*, 449−450). The unusual product was proposed to emanate from trapping of the intermediate with β-mercaptoethanol in competition with hydride transfer from H_4folate to form dTMP. Using mutants of the C-terminal residue of thymidylate synthase, we found that the ratio of HETM-dUMP to dTMP varies as a function of CH_2H_4folate concentration. This observation seemed inconsistent with the conclusion that both products arose from a common intermediate in which CH_2H_4folate was already bound to the enzyme. The enigma was resolved by a kinetic model that allowed for differential partitioning of the intermediate formed on each of the two subunits of the homodimeric enzyme in forming the two different products. With three C-terminal mutants of *L. casei* TS, HETM-dUMP formation was consistent with a model in which product formation occurs upon occupancy of the first completely bound subunit, the rate of which is unaffected by occupancy of the second subunit. With one analogous *E. coli* TS mutant, HETM-dUMP formation occurred upon occupancy of the first subunit, but was inhibited when both subunits were occupied. With all mutants, dTMP formation occurs from occupied forms of both subunits at different rates; here, binding of cofactor to the first subunit decreased affinity for the second, but the reaction occurred faster in the enzyme form with both subunits bound to dUMP and CH_2H_4folate. The model resolves the apparent enigma of the cofactor-dependent product distribution and supports the conclusion that the exocyclic methylene intermediate is common to both HETM-dUMP and dTMP formation.

Thymidylate synthase (TS,[1] EC 2.1.1.45) catalyzes the conversion of dUMP and 5,10-methylene-5,6,7,8-tetrahydrofolate (CH_2H_4folate) to dTMP and 7,8-dihydrofolate (H_2-folate). In all cases examined, TS is a highly conserved dimer of identical subunits; the enzyme has been extensively studied in terms of structure, mechanism, and mutagenesis (*1*).

† This work was supported by USPHS Grant CA14394. T.T.L. is supported by USPHS Grant CA 41323.

* To whom correspondence should be addressed. Phone: (415) 476-1740. Fax: (415) 476-0473. E-mail: santi@socrates.ucsff.edu.

[1] Abbreviations: TS, thymidylate synthase; CH_2H_4folate, 5,10-methylene-5, 6,7,8-tetrahydrofolate; H_2folate, 7,8-dihydrofolate; dUMP, 2′-deoxyuridine 5′-monophosphate; dTMP, thymidine 5'-monophosphate; HETM-dUMP, 5-(2-hydroxyethyl)thiomethyl-dUMP; TES, *N*-[tris[hydroxymethyl]methyl]-2-aminoethanesulfonic acid; βME, β-mercaptoethanol; HPLC, high-performance liquid chromatography; TBAHS, tetra-*n*-butylammonium hydrogen sulfate; TFA, trifluoroacetic acid.

10.1021/bi991802d CCC: $19.00
Published on Web 02/16/2000

Scheme 1

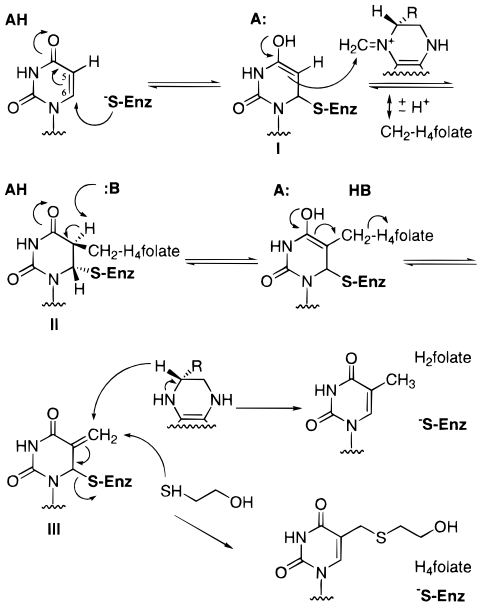

Scheme 2

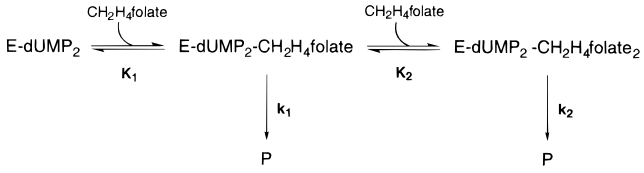

The salient features of the chemical pathway of the TS reaction are shown in Scheme 1. Within the reversible TS−dUMP−CH_2H_4folate complex, nucleophilic attack by the thiol of a cysteine residue (Cys 198 in *Lactobacillus casei* TS[2]) at C-6 of dUMP converts the 5-carbon of dUMP to the enol **I**. This is followed by covalent bond formation between C-5 of dUMP and the one-carbon unit (C-11) of CH_2H_4-folate to produce intermediate **II**. The C-5 proton of **II** is removed, leading to the β-elimination of H_4folate to give the intermediate **III**. Finally, hydride transfer from H_4folate to the exocyclic methylene group of **III** and β-elimination of the enzyme result in the products H_2folate and dTMP.

Direct evidence for the exocyclic intermediate **III** was recently obtained by studies of *L. casei* TS W82 mutants (*2*). These mutants produced 5-(2-hydroxyethyl)thiomethyl-dUMP (HETM-dUMP) in addition to dTMP. It was proposed that the unusual product was derived from trapping of intermediate **III** with β-mercaptoethanol, a component of the assay buffer, in direct competition with the reaction of hydride from H_4folate (Scheme 2). In the course of studies directed at understanding how extensive this reaction was in our library of TS mutants, we observed that the ratio of HETM-dUMP to dTMP varied as a function of CH_2H_4folate concentration. Since this seemed inconsistent with the previous conclusion that HETM-dUMP and dTMP arose from partitioning of the common intermediate **III**, we undertook a more detailed study of the reaction.

In the present work, we investigated the effect of CH_2H_4-folate concentration on the kinetics of HEMT-dUMP and dTMP formation by three C-terminal mutants of *L. casei* TS and one C-terminal mutant of *E. coli* TS. The enigma of cofactor-dependent product distribution was resolved by a model, in which the two subunits of the homodimeric enzyme catalyze formation of the two products at different rates. That is, there is a cofactor-induced nonequivalency of sites that results in different partitioning of intermediate **III** at each of the two subunits.

MATERIALS AND METHODS

Materials. (6*R*)-CH_2H_4folate was a gift from EPROVA AG (Schaffhausen, Switzerland). pThyA containing the *E. coli* TS gene was originally a gift from Frank Maley, New York Department of Public Health, Albany, NY. (*3*). Unless otherwise specified, all materials were obtained from commercial sources.

TS Mutants. The *L. casei* TS mutants V316Am, V316G, V316R, and W82Y have been previously described (*4*, *5*). *E. coli* I264Am was prepared by mutagenesis of pThyA using the QuikChange site-directed mutagenesis kit (Stratagene, La Jolla, CA) with 5′-GGCATTAAAGCGCCGGTGGCT-TAGTAATTACGAAACATCC-3′ and its reverse complement as mutagenic primers; the underlined TAG amber codon replaces the wild-type ATC. The resultant pThyA (I264Am) was used to transform *E. coli* strain χ2913recA (*4*), and the colonies resistant to ampicillin were selected (*6*). The mutation was confirmed by sequencing.

For expression and purification of I264Am, a single colony was inoculated into 100 mL of LB containing 50 μg/mL ampicillin, and after growth at 37 °C overnight, the culture was transferred to 4 L of LB containing 50 μg/mL ampicillin. Cells were harvested by centrifugation at 5000 rpm for 10 min and lysed by sonication, and the protein was purified by a modification of the procedure described for wild-type *E. coli* TS (*3*). After the phenyl sepharose procedure, about 5 mg of the total protein was applied to a POROS 20 HQ column (4.6 × 50 mm) previously equilibrated with 25 mM phosphate, pH 7.5, containing 20 mM βME. The enzyme was eluted using an 18 mL gradient of 0−0.6 M NaCl in 25 mM phosphate containing 20 mM βME, pH 7.5. The recovered protein (∼4 mg) was >95% homogenous by SDS−PAGE. The total yield of pure I264Am from 4 L of culture was ∼100 mg.

TS HPLC Assay. Reaction mixtures (500 μL) contained 250 μM dUMP, varying concentrations of (6*R*)-CH_2H_4folate, and 4.0 μM *L. casei* TS V316Am or a 1.0 μM concentration of other mutants in TES buffer (50 mM TES, 25 mM $MgCl_2$, 6.5 mM formaldehyde, 1 mM EDTA, 75 mM βME, pH 7.4). After 150 min for *L. casei* mutants or 60 min for *E. coli* I264Am, reactions were quenched by the addition of 30 μL of 20% TCA (w/v). Following centrifugation at 10 000 rpm for 10 min, the supernatant was neutralized by vortexing with an equal volume of 0.5 M tri-*n*-octylamine in dichloromethane (*7*). The aqueous layer was collected, and a 200 μL aliquot was chromatographed on a Beckman Ultrasphere IP column (4.6 × 250 mm) using a Hewlett-Packard 1090 HPLC equipped with a diode array detector. Solvent A was 5 mM KH_2PO_4 (pH 7.0) containing 5 mM TBAHS, and solvent B was a 1:1 mixture of 10 mM KH_2PO_4 (pH 7.0) containing 10 mM TBAHS and 100% acetonitrile. A gradient of 0−20 % B was achieved in 30 min and 20−30% B in

[2] TS amino acids are numbered appropriately for each source; V316 of *L. casei* TS corresponds to I264 of *E. coli* TS.

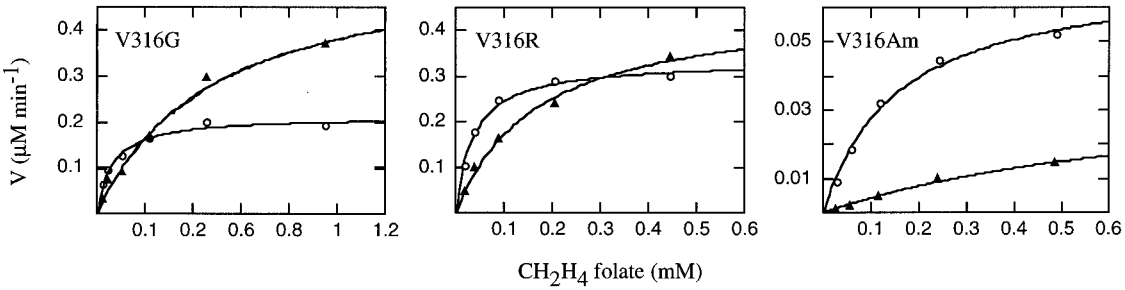

FIGURE 1: Rate of formation of dTMP (▲) and HETM-dUMP (○) *versus* the concentration of CH_2H_4 folate at 250 μM dUMP for V316G, R, and Am. Data were fit using the Henri−Michaelis−Menten equation for a single-site system.

another 10 min. Each peak was scanned from 220 to 400 nm and identified by its retention time (dUMP, 17.5 min; dTMP, 21 min; HETMdUMP, 27 min), λ_{max} (dUMP, 263 nm; dTMP, 269 nm; HETM-dUMP, 270 nm), and comigration with authentic standards. Nucleotide concentrations were determined by integrating the area under the peak at 265 nm and comparison to calibration standards.

The CH_2H_4folate concentration (S) at the time of measurement (t) was calculated by subtracting the dTMP formed from the initial cofactor concentration (S_0). Note that HETM-dUMP formation is not accompanied by CH_2H_4folate consumption; rather, H_4folate is formed, which is recycled to CH_2H_4folate in the presence of the excess formaldehyde. The average CH_2H_4folate concentration over the rate measurement was calculated as $(S_0 + S)/2$, and the overall rate was calculated as $(S_0 - S)/t$. For kinetic analysis, average CH_2H_4-folate concentrations and overall rates were calculated for each data point and used in fitting the data to the appropriate equation (*8*).

Preparation of HETM-dUMP. A solution (8 mL) containing TES buffer, 1.25 mM dUMP, 1.25 mM CH_2H_4folate, and 13.5 μM W82Y was incubated at room temperature overnight. After TCA precipitation of protein, the products were isolated as described above. The aqueous layer was applied to a DE52 column (20 mL) equilibrated with 5 mM ammonium bicarbonate. After the column was washed with the same buffer, nucleotides were eluted with a 200 mL linear gradient of 10−100 mM ammonium bicarbonate. HETM-dUMP was further purified by chromatography on a Vydac C-18 HPLC column (10 × 250 mm) with solvent A as 0.1% TFA in H_2O and solvent B as 80% acetonitrile plus 20% A, using a linear gradient of 0−20% B in 20 min. The ^{1}H NMR of the purified HETM-dUMP was identical to that reported (*2*).

The concentration of HETM-dUMP was determined spectrophotometrically, assuming a ϵ_{max} identical that of to dTMP ($\epsilon_{270} = 9650\ M^{-1}\ cm^{-1}$). Known concentrations of HETM-dUMP (0.050−6.4 nmol in 200 μL) were injected onto a Beckman Ultrasphere IP column (4.6 × 250 mm) and the peak areas at 265 nm determined. A calibration curve of HETM-dUMP versus peak area served to estimate the concentration of nucleotides in the samples following HPLC separations.

Stability of HETM-dUMP in the Presence of V316G and H_4folate. A solution (500 mL) containing TES buffer, 200 mM HETM-dUMP, 200 mM H_4folate, and 10 mM V316G was incubated at room temperature for 16 h. After removal of the protein and neutralization as described above, the products were subjected to HPLC analysis.

Data Processing. Kinetic and thermodynamic parameters were determined by nonlinear least-squares fits of data to the appropriate equations using the program KaleidoGraph 3.0.2 (Abelbeck Software) run on a Macintosh Power PC.

RESULTS AND DISCUSSION

L. casei C-Terminal Mutants. Development of the Model. Three TS V316 mutants were chosen for the present work: V316G, V316R, and V316Am. dTMP and HETM-dUMP, and only these products, were produced by each of the mutants, but in different relative amounts. Under saturating concentrations of dUMP and CH_2H_4folate, HETM-dUMP represents a small amount of the total product with V316G (34%), a moderate amount with V316R (44%), and a large amount with V316Am (78%).

In early experiments we demonstrated that the HETM-dUMP/dTMP formed was constant over time and varying dUMP concentration (data not shown). However, the HETM-dUMP/dTMP was affected by CH_2H_4folate concentration. Figure 1 shows the initial rates of formation of dTMP and HETM-dUMP for the three mutants studied under conditions of saturating dUMP concentration and varying concentrations of CH_2H_4folate. In all cases, the apparent CH_2H_4folate K_m values for HETM-dUMP formation are lower than those for dTMP formation, and the rate of formation of HETM-dUMP achieved saturation at lower cofactor concentration than that of dTMP. Further, in all mutants the initial rate of HETM-dUMP formation at low cofactor concentrations appears to be greater than that of dTMP formation, although with two mutants (V316G, V316R) the V_{max} is lower. Interestingly, V316Am, which produces dTMP very slowly, produces a relatively large amount of HETM-dUMP.

The formation of dTMP and H2folate is energetically favorable and essentially irreversible (*1*, *9*). However, there is no *a priori* reason to believe that the reaction of intermediate **III** with βME to give HETM-dUMP and H_4folate would be irreversible. It was considered possible that at low cofactor concentrations, H_4folate would irreversibly escape from the enzyme after HETM-dUMP formation, whereas with high cofactor concentrations, the increased H_4folate present in equilibrium with CH_2H_4folate might effectively reverse the reaction and result in an increased partitioning of **III** to dTMP. If correct, the folate dependence of the HETM-dUMP/dTMP might simply be explained by product inhibition. To test this possibility, we prepared HETM-dUMP and examined its ability to undergo a reverse reaction with H_4folate to form dUMP or dTMP. When 200 μM HETM-dUMP and 200 μM H_4folate were treated with V316G for 20 h, HPLC analysis showed no new nucleotide peaks. Thus,

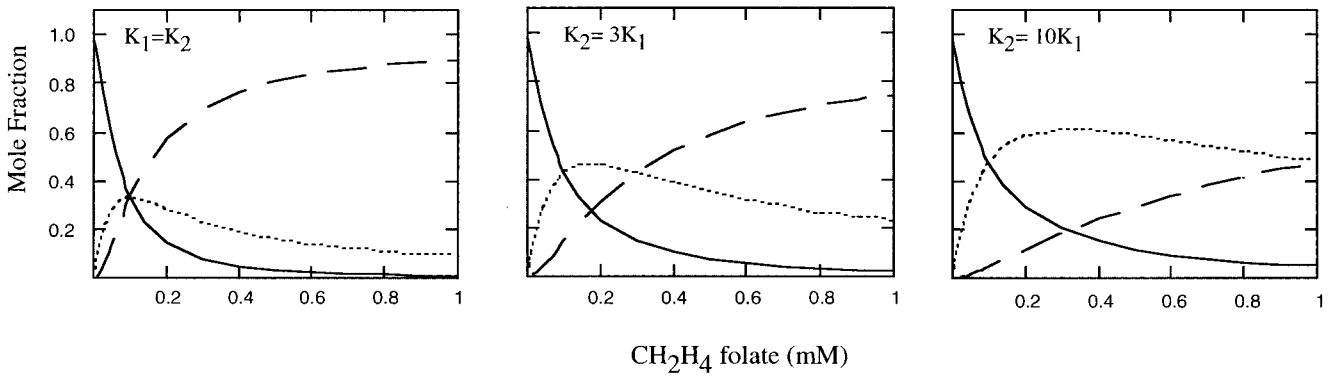

FIGURE 2: Simulation of the mole fractions of various enzyme forms as a function of CH_2H_4 folate concentration. The three panels show the relative population of enzyme forms with different K_2 values (A, 0.1 mM; B, 0.3 mM; C, 1 mM) at a fixed value of K_1 (0.1 mM). The solid line represents E−dUMP$_2$, the dotted line E−dUMP$_2$−CH_2H_4folate, and the dashed line E−dUMP$_2$−CH_2H_4folate$_2$.

under the experimental conditions used here, the formation of HETM-dUMP and H_4folate is effectively irreversible, and the reverse reaction does not account for the cofactor-dependent change in HETM-dUMP/dTMP.

It has been well established that the two subunits of the homodimeric TS are occupied by both substrates, although binding to the first decreases, and under some conditions prevents, binding of the second (*9*−*14*). Regardless, others and we have usually assumed a conventional single (or independent equivalent) site system for kinetic analysis because the different sites are sufficiently similar that kinetic differences are not easily resolved. Scheme 2 shows the two-subunit model pathway we have used to describe the TS-catalyzed formation of dTMP and HETM-dUMP; the model is depicted and analyzed under conditions of saturating dUMP concentration and varying concentrations of CH_2H_4folate. E−dUMP$_2$ represents the heterodimer saturated with dUMP but not containing CH_2H_4folate, E−dUMP$_2$−CH_2H_4folate is the form with both subunits occupied by dUMP and a single subunit site occupied by CH_2H_4folate, and E−dUMP$_2$-CH_2H_4folate$_2$ is the form with both sites occupied by both dUMP and CH_2H_4folate. In this model, K_1 and K_2 are K_m values assumed to be dissociation constants for the referred-to enzyme forms, and k_1 and k_2 represent the k_{cat} values for the formation of either product by E−dUMP$_2$−CH_2H_4folate and E−dUMP$_2$−CH_2H_4folate$_2$, respectively. Figure 2 shows simulations of concentrations of the three enzyme forms as a function of CH_2H_4folate concentration assuming $K_1 = K_2$, $K_2 = 3K_1$, and $K_2 = 10K_1$. Here, *E*−dUMP$_2$−CH_2H_4folate increases to a maximum when $K_1 < [CH_2H_4\text{folate}] < K_2$, then decreases, and approaches zero as $[CH_2H_4\text{folate}] > K_2$, and E−dUMP$_2$−$CH_2H_4$folate$_2$ predominates over other enzyme forms. It can be seen from Figures 1 and 2 that E−dUMP$_2$−CH_2H_4folate is not the sole reactive form for dTMP or HETM-dUMP formation; otherwise, the V_{max} values would decrease at high cofactor concentrations.

The assumptions and tenets used in the ensuing analysis are as follows. First, as previously proposed (*2*) both dTMP and HETM-dUMP emanate from partitioning of the covalent ternary complex **III**, so the formations of both products have the same pathway up to and including formation of the intermediate.[3] Second, both bound enzyme forms are active in producing either product; thus, the apparent K_m and k_{cat} values obtained by a single-site model are each composed of two unresolved microscopic constants. Third, we assume that k_{cat} for either product is rate determining (i.e., preequilibrium formation of reversibly bound enzyme forms), as shown for dTMP formation with wild-type *E. coli* enzyme (*1*, *9*). Thus, the rate of formation of either product as described by eq 1 expands into one for the rapid-equilibrium mechanism in eq 2. Here, the formation of products is described as a function of the dissociation (K) and rate (k) constants, and K_m values reflect dissociation constants of the cofactor.

$$v = k_1[\text{E}-\text{dUMP}_2-\text{CH}_2\text{H}_4\text{folate}] + k_2[\text{E}-\text{dUMP}_2-\text{CH}_2\text{H}_4\text{folate}_2] \quad (1)$$

$$v = \left[\frac{k_1}{K_1/[\text{CH}_2\text{H}_4\text{folate}] + 1 + [\text{CH}_2\text{H}_4\text{folate}]/K_2} + \frac{k_2}{K_1K_2/[\text{CH}_2\text{H}_4\text{folate}]^2 + 1 + K_2/[\text{CH}_2\text{H}_4\text{folate}]}\right][\text{E}_t] \quad (2)$$

Since the K_1 and K_2 values for cofactor binding must be the same for both reactions, and since the HETM-dUMP reaction shows a lower apparent K_m than dTMP formation, we conclude that the HETM-dUMP K_m reflects K_1 and the apparent dTMP K_m reflects a composite of and lies between K_1 and K_2. Importantly, rate saturation for HETM-dUMP formation occurs in apparent accord with occupancy of a single site; however, as previously argued, the reaction cannot

[3] A reviewer suggested a model in which H_4folate dissociates from the enzyme−exocyclic methylene intermediate before 2-mercaptoethanol enters to react with it. The increased H_4folate present in equilibrium at higher cofactor concentrations would result in higher occupancy of the complex, which might explain increased partitioning of the intermediate toward dTMP at high cofactor concentration. If correct, exogenous H_4folate would have the same effect. TS W82A was treated with 30 mM cofactor, 250 mM dUMP, and varying H_4folate concentration without added formaldehyde, and the dTMP and HETM-dUMP were measured. With increasing H_4folate concentration, the rate of product formation decreased in accord with competitive inhibition with a K_i of about 150 mM. However, over a range of 15−125 mM H_4folate the dTMP/HETM-dUMP remained constant at 1.25. This result argues against the suggestion that increased partitioning toward dTMP results from loss of H_4folate from the enzyme−exocyclic methylene intermediate.

Table 1: Kinetic Parameters for HETM-dUMP and dTMP Formation

	HETM-dUMP				dTMP				
TS	k_1[a] (min^{-1})	k_2[b] (min^{-1})	K_1[c] (μM)	K_2 (μM)	k_1[a] (min^{-1})	k_2[b] (min^{-1})	$K_{m,app}$[d] (μM)	K_1[c] (μM)	K_2 (μM)
V316G	0.22 (0.25)	0.22	73	*e*	0.074 (0.078)	0.59	554	73	626
V316R	0.30 (0.36)	0.35	54	*e*	0.11 (0.11)	0.52	249	54	322
V316Am	0.070 (0.061)	0.070	160	*e*	0.007 (*f*)	0.04	848	163	953
I264Am	0.34−0.35 (0.50)	0−0.0034	29−30	270−280	0.34−0.35 (0.27)	1.32	144	29−30	216−220

[a] Parenthesized k_1 values were experimentally obtained by extrapolating plots of S/v versus S to $S = 0$ to give K_m/V_{max} (*8*). [b] The k_2 values for HETM-dUMP formation with *L. casei* mutants and for dTMP formation are k_{cat} values derived from V_{max} values; for *E. coli* I264Am-catalyzed HETM-dUMP formation, the range of k_2 is the best fit within limits set by experimental data. [c] For *L. casei* mutants, K_1 is the K_m for the cofactor obtained from fits of the data for HETM-dUMP formation to the Michaelis−Menten equation. For *E. coli* I264Am, K_1 was determined by the best fit of the data for HETM-dUMP formation to eq 2 as described in the text. [d] The apparent cofactor K_m values for dTMP formation are from best fits of the data to the Michaelis−Menten equation for a single-site system. Other constants were obtained by best fits of the data to eq 2 with constraints as described in the text. [e] Undeterminable with the current data. [f] The rate was too slow to obtain a reliable experimental estimate.

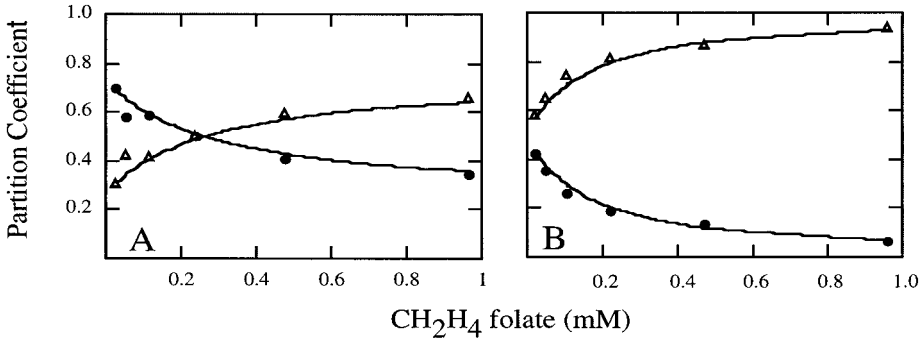

FIGURE 3: Partitioning of intermediate **III** to HETM-dUMP in (A) *L. casei* V316G and (B) *E. coli* I264Am at different CH_2H_4folate concentrations. Experimental values are shown for HETM-dUMP (●) and dTMP (△), and the solid lines are calculated from eq 3 using values from Table 1. For *E. coli* mutant the solid line indicates calculated values using $k_1 = 0.34$, $k_2 = 0.0034$, and $K_2 = 268$ μM for HETM-dUMP formation and $k_1 = 0.35$, $k_2 = 1.31$, and $K_2 = 268$ μM for dTMP formation.

occur solely from the enzyme form with single-subunit occupancy; otherwise, the concentration of E−dUMP$_2$−CH_2H_4folate and therefore the reaction rate would decrease at high cofactor concentration. To explain this apparent enigma in context of the enzyme forms present under varying cofactor concentration (Figure 2, Scheme 2), k_1 must be equal to k_2 for HETM-dUMP formation; in effect, occupancy of the second subunit by both substrates does not affect the rate of HETM-dUMP formation. As indicated in Figure 2, if k_2 were lower than k_1, at high concentrations of CH_2H_4-folate, E−dUMP$_2$−CH_2H_4folate$_2$ would predominate and the rate would decrease; if k_2 were greater than k_1, at high concentrations of CH_2H_4folate, E−dUMP$_2$−CH_2H_4folate$_2$ would predominate and the rate would increase. Since neither is the case, we conclude that $k_1 = k_2$ for HETM-dUMP formation.

From the rate dependence of HETM-dUMP formation *versus* [CH_2H_4folate] (Figure 1), we directly obtained K_1 (K_m) and k_2 (from V_{max}). With these constants as constraints, best fits of the data for HETM-dUMP formation to eq 2 showed that k_1 values were essentially identical to k_2 (Table 1). As expected, since $k_1 = k_2$, k_1 values were insensitive to K_2 values used in eq 2.

In dTMP formation, both sites are active and the apparent K_m for the cofactor is a composite of K_1 and K_2. To fit the experimental data to eq 2, we used the K_1 value measured from HETM-dUMP formation and k_2 from the V_{max} of dTMP formation (Figure 1). Using K_1 and k_2 as constraints, best fits of the data to eq 2 yielded the values for k_1 and K_2 given in Table 1. Experimentally determined values of k_1 obtained by extrapolating plots of S/v *versus* S to zero cofactor concentration (*8*) were in excellent agreement with those obtained from eq 2. It is noted that the data for dTMP formation can be fit equally well ($R^2 = 0.99$) to eq 2 or the Henri−Michaelis−Menten equation for a single (or two equivalent independent) site(s) ($R^2 = 0.99$), and in the absence of other information the differential activity of the two sites cannot be resolved.

The partition coefficient of intermediate **III**, $k_{HETM-dUMP}/(k_{HETM-dUMP} + k_{dTMP})$, from either of the two reactive enzyme forms may be calculated from the values in Table 1. The partitioning of **III** in the fully occupied enzyme can also be experimentally determined as the fraction of HETM-dUMP (i.e., HETM-dUMP/[HETM-dUMP + dTMP]), formed at saturating cofactor concentrations where all enzyme is present as E−dUMP$_2$−CH_2H_4folate$_2$. Finally, the fraction of **III** simultaneously formed from all enzyme forms at any concentration of the cofactor may be calculated by using eq 3 and the constants given in Table 1. As shown in Figure 3, there is excellent agreement between values calculated from eq 3 and the experimental data obtained at varying cofactor concentrations.

$$([\text{dTMP}])/([\text{HETM-dUMP}] + [\text{dTMP}]) = [K_2[\text{CH}_2\text{H}_4\text{folate}]k_{1(\text{dTMP})} + [\text{CH}_2\text{H}_4\text{folate}]^2 k_{2(\text{dTMP})}]/[K_2[\text{CH}_2\text{H}_4\text{folate}](k_{1(\text{dTMP})} + k_{1(\text{HETM-dUMP})}) + [\text{CH}_2\text{H}_4\text{folate}]^2(k_{2(\text{dTMP})} + k_{2(\text{HETM-dUMP})})] \quad (3)$$

E. coli I264Am. Verification of the Model. We felt that structural studies of a mutant that produced HETM-dUMP might reveal information regarding how this unusual product

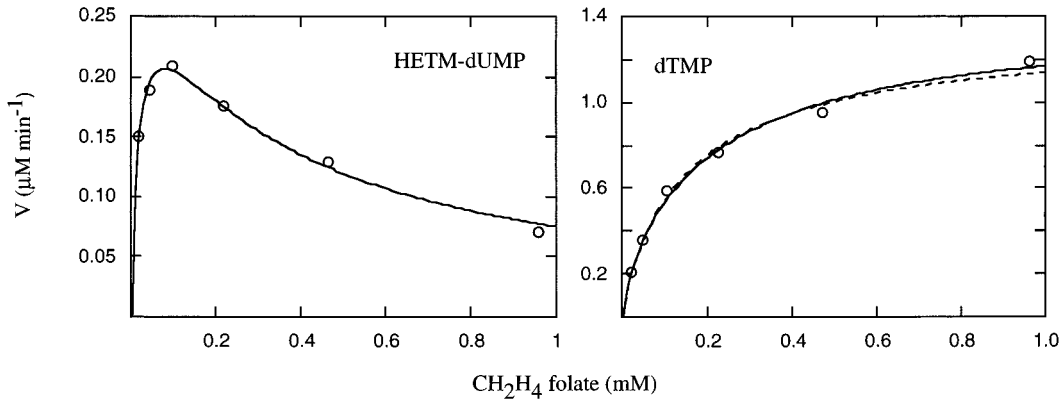

FIGURE 4: Rate of I264Am-catalyzed formation of HETM-dUMP and dTMP *versus* CH_2H_4folate concentration. For HETM-dUMP formation, data were fit to eq 2 assuming $k_2 = 0$. For dTMP formation, data were fit to eq 2 as described in the text; (dotted line, k_2 and K_1 as constraints; solid line, K_1 and K_2 as constraints). Points are experimental data.

was formed. Of the mutants described thus far, *L. casei* TS V316Am produced the largest amount of HETM-dUMP over dTMP, and thus seemed an appropriate candidate for structure determination. We prepared the corresponding *E. coli* TS I264Am since ternary complexes of the *E. coli* enzyme have been found to be more amenable to crystallization (*15*). However, kinetic characterization of the mutant revealed properties different from those observed with the corresponding *L. casei* mutant.

At saturating cofactor concentration, *E. coli* TS I264Am was ~30-fold more active at dTMP production than *L. casei* TS V316Am but much less efficient at HETM-dUMP production (Table 1). Moreover, with varying cofactor concentration the rate of HETM-dUMP formation increased to a maximum at about 100 μM CH_2H_4folate and then decreased with increasing concentrations (Figure 4). Comparison of Figure 4 to Figure 2 shows that with varying cofactor concentration the *E. coli* TS I264Am-catalyzed formation of HETM-dUMP tracks the enzyme form occupied at a single subunit, $E-(dUMP)_2-CH_2H_4$folate. The data were fit to eq 2 by constraining k_2 over the range of $0-0.07$ min^{-1}; the latter is the last data point sampled, and represents an upper limit. The best fits ($R^2 \geq 0.99$) occurred with $k_1 = 0.34$, $k_2 = 0-0.003$, $K_1 = 29-30$ μM, and $K_2 = 270$ to 280 μM. The k_1 obtained is in excellent agreement with the experimentally determined value obtained by a plot of S/v vs S (0.38 min^{-1}). Thus, with *E. coli* I264Am, $E-dUMP_2-CH_2H_4$folate is active in the formation of HETM-dUMP, but in contrast to the corresponding *L. casei* TS mutant, full occupancy of both subunits causes a complete or near-complete inhibition of the reaction (i.e., $k_2 = 0-0.003$). The differential behavior of the fully occupied enzyme forms of the *E. coli* and *L. casei* C-terminal deletion mutants in HETM-dUMP formation, together with their excellent fits to eq 2, adds credence to the model proposed in Scheme 2.

dTMP formation by *E. coli* TS I264Am behaved as did the *L. casei* TS mutants, with both sites active in forming product. The rate data were fit to eq 2 by constraining K_1 to the range obtained for HETM-dUMP formation and to the k_2 for dTMP formation ($R^2 = 0.99$; Figure 4). The K_2 and k_1 values thus obtained were $216-220$ μM and $0.34-0.35$ min^{-1}, respectively. When eq 2 was constrained by K_1 and K_2 obtained from HETM-dUMP formation, the fit was also excellent ($R^2 = 0.99$) and the calculated values were in agreement with those reported above ($k_1 = 0.4$, $k_2 = 1.4$ min^{-1}; Figure 4). The apparent K_m for dTMP using a single-site model (144 μM) lies intermediate to the two microscopic dissociation constants K_1 and K_2. Finally, for *E. coli* I264Am, the partitioning of **III** to products at any cofactor concentration calculated from eq 3 is in excellent agreement with the experimental data (Figure 3, panel B).

SUMMARY

Using data obtained from three C-terminal *L. casei* TS mutants and one analogous *E. coli* TS mutant, we constructed a congruent model for the reaction pathways leading to the formation of HETM-dUMP and dTMP. The model embraces the original proposal that the two products emanate from a common steady-state intermediate (*2*). It explains the cofactor dependence of the relative amounts of products formed by different partitioning of the steady-state intermediate **III** in forms of the homodimeric enzyme that are occupied by substrates at one *versus* two subunits. In the case of *L. casei* V316 mutants, HETM-dUMP formation can be explained by a model in which the unusual product forms upon occupancy of the first bound subunit, and the rate is unaffected by occupancy of the second. For *E. coli* TS I264Am, HEMTM-dUMP is formed upon occupancy of the first bound subunit, but is inhibited by occupancy of the second. For all mutants studied, dTMP formation emanates from occupied forms of both subunits at different rates; there is a cooperative effect in which binding of cofactor at the first subunit decreases binding to the second, and the reaction occurs ~4−8-fold faster in the completely occupied enzyme form. Utilizing the K_1 values obtained from HETM-dUMP formation with these TS mutants enabled resolution of differences in the kinetic parameters of the two subunits in dTMP formation that are not easily determined by conventional steady-state kinetic analysis. Indeed, we can confidently assign the different rate and cofactor binding constants associated with the singly and fully occupied subunit forms of the homodimeric enzyme. Further, the approach should be generally applicable to other heterodimeric systems (e.g., wild-type TS and other mutants), provided an independent method is available to determine K_1. With the ability to dissect the dependency of product formation *versus* cofactor concentration, we are now in a

position to proceed with studies directed toward further understanding the mechanistic details of HETM-dUMP formation in various TS mutants.

ACKNOWLEDGMENT

We thank Dr. Patricia Greene and Thomas Ba for their helpful suggestions.

APPENDIX

The derivation of eq 2 is based on the pathway shown in Scheme 2 and assumes a rapid equilibrium of enzyme forms prior to a rate-determining catalytic reaction. The potentially reactive enzyme forms were defined in terms of dissociation constants

$$K_1 = \frac{[\text{E}-\text{dUMP}_2][\text{CH}_2\text{H}_4\text{folate}]}{[\text{E}-\text{dUMP}_2-\text{CH}_2\text{H}_4\text{folate}]}$$

$$K_2 = \frac{[\text{E}-\text{dUMP}_2-\text{CH}_2\text{H}_4\text{folate}][\text{CH}_2\text{H}_4\text{folate}]}{[\text{E}-\text{dUMP}_2-\text{CH}_2\text{H}_4\text{folate}_2]}$$

and the total enzyme was described as the sum of all enzyme forms

$$[\text{E}_t] = [\text{E}-\text{dUMP}_2] + [\text{E}-\text{dUMP}_2-\text{CH}_2\text{H}_4\text{folate}] + [\text{E}-\text{dUMP}_2-\text{CH}_2\text{H}_4\text{folate}_2]$$

The potentially reactive enzyme forms were described in terms of the total enzyme, dissociation constants, and cofactor concentration

$$[\text{E}-\text{dUMP}_2-\text{CH}_2\text{H}_4\text{folate}]/[\text{E}_t] = \frac{1}{K_1/[\text{CH}_2\text{H}_4\text{folate}] + 1 + [\text{CH}_2\text{H}_4\text{folate}]/K_2} \quad (4)$$

$$[\text{E}-\text{dUMP}_2-\text{CH}_2\text{H}_4\text{folate}_2]/[\text{E}_t] = \frac{1}{K_1K_2/[\text{CH}_2\text{H}_4\text{folate}]^2 + 1 + K_2/[\text{CH}_2\text{H}_4\text{folate}]} \quad (5)$$

These expanded equations were substituted into the rate expression

$$v = k_1[\text{E}-\text{dUMP}_2-\text{CH}_2\text{H}_4\text{folate}] + k_2[\text{E}-\text{dUMP}_2-\text{CH}_2\text{H}_4\text{folate}_2] \quad (1)$$

to give eq 2.

$$v = \left[\frac{k_1}{K_1/[\text{CH}_2\text{H}_4\text{folate}] + 1 + [\text{CH}_2\text{H}_4\text{folate}]/K_2} + \frac{k_2}{K_1K_2/[\text{CH}_2\text{H}_4\text{folate}]^2 + 1 + K_2/[\text{CH}_2\text{H}_4\text{folate}]}\right][\text{E}_t] \quad (2)$$

REFERENCES

1. Carreras, C. W., and Santi, D. V. (1995) *Annu. Rev. Biochem. 64*, 721−762.
2. Barrett, J. E., Maltby, D. A., Santi, D. V., and Schultz, P. G. (1998) *J. Am. Chem. Soc. 120*, 449−450.
3. Maley, G. F., and Maley, F. (1988) *J. Biol. Chem. 263*, 7620−7.
4. Climie, S. C., Carreras, C. W., and Santi, D. V. (1992) *Biochemistry 31*, 6032−6038.
5. Kealey, J. T., Eckstein, J., and Santi, D. V. (1995) *Chem. Biol. 2*, 609−614.
6. Maniatis, T., Fritsch, E. F., and Sambrook, J. (1982) *Molecular cloning: a laboratory manual*, Cold Spring Harbor Laboratory, Cold Spring Harbor, NY.
7. Pogolotti, A. L., and Santi, D. V. (1982) *Anal. Biochem. 126*, 335−345.
8. Segel, I. H. (1975) *Enzyme Kinetics: Behavior and Analysis of Steady-State and Rapid Equilibrium Enzyme Systems*, pp 57−58 and 210, Wiley-Interscience, New York.
9. Spencer, H. T., Villafranca, J. E., and Appleman, J. R. (1997) *Biochemistry 36*, 4212−4222.
10. Sage, C. R., Rutenber, E. E., Stout, T. J., and Stroud, R. M. (1996) *Biochemistry 35*, 16270−81.
11. Stout, T. J., and Stroud, R. M. (1996) *Structure 4*, 67−77.
12. Galivan, J. H., Maley, G. F., and Maley, F. (1976) *Biochemistry 15*, 356−62.
13. Dev, I. K., Dallas, W. S., Ferone, R., Hanlon, M., McKee, D. D., and Yates, B. B. (1994) *J. Biol. Chem. 269*, 1873−1882.
14. Lockshin, A., Mondal, K., and Danenberg, P. V. (1984) *J. Biol. Chem. 259*, 11346−11352.
15. FinerMoore, J. S., Liu, L., Birdsall, D. L., Brem, R., Apfeld, J., Santi, D. V., and Stroud, R. M. (1998) *J. Mol. Biol. 276*, 113−129.

BI991802D